

# An in Vitro Study of the Effect of Mage-D1 in Rat Dental Mineralization via Dynamic Histology and Ectomesenchymal Stem Cell

**Meng Li**

Chongqing Key Laboratory of Oral Diseases and Biomedical Sciences, Chongqing Municipal Key Laboratory of Oral Biomedical Engineering of Higher Education, Chongqing

**Xia Yu**

Department of Orthodontics, Hospital of Stomatology, Southwest Medical University, Luzhou, Sichuan

**Yuting Luo**

Stomatological Hospital of Chongqing Medical University

**Hongyan Yuan**

Department of Orthodontics, Hospital of Stomatology, Southwest Medical University, Luzhou, Sichuan

**Yixing Zhang**

Department of Orthodontics, Hospital of Stomatology, Southwest Medical University, Luzhou, Sichuan

**Xiujie Wen**

Department of Orthodontics, Hospital of Stomatology, Southwest Medical University, Luzhou, Sichuan

**Zhi zhou** (✉ [500119@hospital.cqmu.edu.cn](mailto:500119@hospital.cqmu.edu.cn))

Stomatological Hospital of Chongqing Medical University

---

## Research Article

### Keywords:

**Posted Date:** February 28th, 2022

**DOI:** <https://doi.org/10.21203/rs.3.rs-1309598/v1>

**License:**  This work is licensed under a Creative Commons Attribution 4.0 International License.

[Read Full License](#)

**Additional Declarations:** No competing interests reported.

---

**Version of Record:** A version of this preprint was published at Scientific Reports on December 30th, 2022. See the published version at <https://doi.org/10.1038/s41598-022-27197-5>.

# Abstract

Mage-D1 (MAGE family member D1) is involved in a variety of cell biological effects. Recent studies have shown that Mage-D1 is closely related to tooth development, but its specific regulatory mechanism is unclear. The purpose of this study was to investigate the expression pattern of Mage-D1 in rat tooth germ development and its differential mineralization ability to ectomesenchymal stem cells (EMSCs), and to explore its potential mechanism. Results showed that the expression of Mage-D1 during rat tooth germ development was temporally and spatially specific. Mage-D1 promotes the proliferation ability of EMSCs but inhibits their migration ability. Under induction by mineralized culture medium, Mage-D1 promotes osteogenesis and tooth-forming ability. In vitro, Mage-D1 not only binds to p75 neurotrophin receptor (p75NTR) but also to distal-less homeobox 1 (Dlx1) and msh homeobox 1 (Msx1). These findings indicate that Mage-D1 is absolutely important in tooth germ development. p75NTR, Dlx1, and Msx1 seem to be closely related to the underlying mechanism of Mage-D1 action.

## Introduction

Teeth, composed of three mineralized tissues (dentine, cementum, and enamel), constitute important models for gaining insight into the general processes of biological mineralization. Both cell-derived microstructures and extracellular matrix components play critical roles in the preorganization and oriented deposition of calcium phosphate and serve as passive supports in dentine and enamel. However, the mechanism of dental mineralization is still far from being revealed, which restricts the process of dental tissue engineering and tooth regeneration. Ectomesenchymal stem cells (EMSCs) derived from the cranial neural crest are significant in tooth development and dental mineralization. The development of teeth is initiated by epithelial–mesenchymal interactions, which form dental papilla cells and dental sac cells, subsequently forming pulp, dentin, cementum, periodontal ligament and proper alveolar bone, except enamel<sup>1–4</sup>. In our previous studies, EMSCs were obtained from rat embryonic facial process tissue by fluorescence p75 neurotrophin receptor (p75NTR) activated cell sorting, providing a good stem cell model for studies of dental mineralization. Further studies confirmed that p75NTR participates in the regulation of tooth development maybe by changing the activity of the key factor distal-less homeobox/msh homeobox (Dlx/Msx), and melanoma-associated antigen D1 (Mage-D1) seems to be play a role in the differentiation and mineralization of EMSCs<sup>5,6</sup>.

Mage-D1, also known as Dlxin-1 or NRAGE, was first cloned and identified as a new member of the type II melanoma-associated antigen gene family by Pold et al. in 1999<sup>7</sup>. Structurally, Mage-D1 possesses the N-terminal sequence Mage homology domain 2 (MHD2), which is a highly conserved structure of the type II Mage gene family. The C-terminal sequence of 220 amino acids is named the Mage homology domain (MHD) and contains 25 repeats of a WQXPXX sequence in the middle region<sup>7–10</sup>. Studies have confirmed that Mage-D1 can interact with a variety of proteins through its three domains<sup>11</sup>. According to reports, Mage-D1 can not only interact with transcription factors (Dlx/Msx<sup>12,13</sup>) but also interact with nuclear

proteins (PCNA<sup>14</sup>, TBX2<sup>15</sup>), cell surface receptors (p75NTR<sup>16</sup>, UNC5H1<sup>17</sup>, ROR2<sup>18</sup>, TrkA<sup>19</sup>) and other proteins involved in cell differentiation, apoptosis, the cell cycle, tumorigenesis and metastasis<sup>20</sup>.

Recently, the effects and mechanism of Mage-D1 in tooth development have been a focus of research. Qi et al. pointed out that Mage-D1 may participate in the proliferation of bone marrow mesenchymal stem cells (BMSCs) and the differentiation of odontoblasts through the NF- $\kappa$ B signalling pathway<sup>21</sup>.

Subsequent studies further confirmed that Mage-D1 inhibits the NF- $\kappa$ B signalling pathway by combining with I $\kappa$ B kinase  $\beta$  (IKK $\beta$ )<sup>22</sup>, which is a vital regulator of odontoblast differentiation. Liu et al. showed that knocking out Mage-D1 can induce the expression of autophagy-related genes by enhancing the activity and differentiation of osteoclasts, thereby accelerating the process of periodontitis<sup>23</sup>. Our previous studies have shown that Mage-D1 could affect the bone differentiation ability of rat EMSCs by binding to p75NTR<sup>5</sup>. All of these studies suggested that Mage-D1 may play an irreplaceable role in the development of teeth.

In this study, to further explore the specific roles of Mage-D1 in tooth development, we first observed the expression pattern of Mage-D1 in rat tooth germ development. Then, we investigated the odontogenesis and mineralization regulation and potential mechanisms of Mage-D1 in vitro through embryonic day 19.5 (E19.5 d) EMSCs.

## Results

### **Haematoxylin-eosin (HE) staining during rat tooth germ development and immunohistochemistry staining for MageD1.**

HE results (Fig. 1a) showed that the end of the tooth plate of the enamel organ swelled into a flower bud shape at E12.5 d, which was the bud stage of tooth germ development. Following E15.5 d, it entered the cap phase, and during this period, it was possible to distinguish the components and supporting tissues of the tooth. Then, E19.5 d entered the bell-shaped period. At this time, the enamel organ was divided into four layers: the outer glaze epithelial layer, the inner epithelial layer, the star network layer and the middle layer. Subsequently, the tooth germ developed continuously, one day after birth (PN1) was in the late bell-shaped stage, and the crown had not yet developed. The morphological development of the PN4 tooth crown was basically complete, the endodermal epithelium was fused at the neck ring, and the epithelial root sheath began to form, which marks the beginning of tooth root development. Immunohistochemistry (Fig. 1b) was used to further observe the expression pattern of Mage-D1 during tooth germ development. During the E12.5 d period, Mage-D1 was strongly expressed in the mesenchyme near the lingual side of the epithelium and the enamel-forming area, and was weakly expressed in the dental follicle but not expressed in the dental papilla. At E15.5 d, Mage-D1 was strongly expressed in the oral epithelium, inner enamel epithelium, outer enamel epithelium and their junctions, and dental follicles. However, it was not obviously expressed in the dental papilla.

Subsequently, the expression of Mage-D1 in tooth germs presented an increasing trend. During the E19.5 d period, Mage-D1 was strongly expressed in the inner enamel epithelium, outer enamel epithelium and their junctions and weakly expressed in the dental papilla. At PN1, Mage-D1 was strongly expressed in

preameloblasts, preodontoblasts, and the apex of the dental papilla, indicating a future mineralization area. During the PN4 period, Mage-D1 was expressed in ameloblasts, odontoblasts, dental follicle cells, alveolar bone osteoblasts, epithelial root sheaths, and enamel matrix but not in early dentin. In conclusion, the expression position of MageD1 on different days of early tooth formation has temporal and spatial specificity and is strongly expressed in ameloblasts and odontoblasts. Both enamel and dentin are mineralized tissues. These results suggested that Mage-D1 may be related to the development of tooth mineralization.

**Isolation and characterization of rat embryonic EMSCs.** SD foetal rats at 19.5 days of pregnancy were obtained, and the maxilla was separated (Fig. 2a). Then, the maxillary tooth germ was obtained, and the EMSCs were successfully isolated and cultured by the tissue block adhesion method (Fig. 2b). The third generation of cells was used for subsequent experiments. The cytoskeleton was stained with phalloidin, which showed that the E19.5 d EMSCs were uniformly long and spindle-shaped and had a fibroblast-like morphology (Fig. 2c). Cell surface antigen was detected by flow cytometry (Fig. 2d). The expression rates of mesenchymal stem cell (MSC) surface markers CD29, CD44, CD90, CD105 and CD146 in E19.5 d EMSCs were 95.25%, 95.01%, 99.51%, 94.96%, and 95.18%, respectively, while the expression rate of the haematopoietic stem cell surface marker CD45 was 0.37%. These results indicated that the cells used in our experiments were MSCs.

**MageD1 inhibits the proliferation and promotes the migration of EMSCs.** We successfully constructed Mage-D1 overexpression and silenced lentivirus-transfected EMSCs in vitro. Immunofluorescence results (Fig. 3a, 3b) showed that the fluorescence staining intensity of MageD1 in the overexpression group was significantly higher than that in the control group. Polymerase chain reaction (PCR) and western blot (WB) results (Fig. 3c, 3d) showed that the expression of MageD1 protein and gene in the overexpression group was significantly higher than that in the control group, and the silencing group was the opposite. The cell counting kit-8 (CCK-8) assay results (Fig. 4a) showed that Mage-D1 positively regulated the proliferation of EMSCs, but further scratch assay results (Fig. 4b, 4c) showed that Mage-D1 negatively regulated the migration of EMSCs.

**MageD1 positively regulates the osteogenesis of EMSCs.** According to reports, Mage-D1 is involved in the development and mineralization of teeth<sup>5</sup>. Therefore, we explored whether Mage-D1 is related to the osteogenesis and odontogenesis of EMSCs. After overexpressing Mage-D1 and culturing with mineralization induction medium, the mRNA levels (Fig. 5a) of mineralization-related factors alkaline phosphatase (ALP), runt-related transcription factor 2 (Runx2), collagen type-1 (Col-1) and odontoblast-like differentiation markers dentin sialophosphoprotein (Dspp) and dentin matrix protein 1 (Dmp1) in EMSCs were increased. The protein levels (Fig. 5b) of Runx2, bonesialoprotein (BSP), osteopontin (OPN), Dspp and Dmp1 were also increased. Further results for both ALP staining (Fig. 5c) to detect mineralization ability and alizarin red staining (Fig. 5d) to detect mineralized knots showed that Mage-D1 enhanced mineralization. At the same time, after we silenced Mage-D1 and cultured it with mineralization induction medium, the results showed that Mage-D1 inhibited the mineralization and osteogenic ability of

EMSCs. Briefly, Mage-D1 is closely related to the development of teeth and positively regulates the osteogenesis and tooth formation ability of EMSCs.

**Potential mechanism of Mage-D1 in regulating mineralization.** Mage-D1 is involved in the tooth formation and osteogenesis process of EMSCs, but its specific mechanism is still unclear. Zhao et al. speculated that Mage-D1 plays a bridge role between the cell membrane receptor p75NTR and the nuclear transcription factor Dlx/Msx<sup>6</sup>. Our immunoprecipitation results (Fig. 6a) showed that Mage-D1 not only binds to p75NTR but also to Dlx1 and Msx1. Further studies have shown that after overexpression of Mage-D1, the gene and protein levels of p75NTR, Dlx1, and Msx1 were increased, after silencing Mage-D1, the gene and protein contents of p75NTR, Dlx1, and Msx1 were decreased (Fig. 6b, 6c). These results suggested that the involvement of Mage-D1 in the process of osteogenesis or tooth formation may be closely related to p75NTR, Dlx1, and Msx1.

## Discussion

Mage-D1 plays an essential role in life activities, including the cell cycle, cell adhesion, cell differentiation, apoptosis, and some tumour events, such as tumour occurrence, invasion, and metastasis<sup>11</sup>. The gene expression profile showed that Mage-D1 was strongly expressed in dental papilla and enamel epithelium, suggesting that Mage-D1 is closely related to tooth development. Our research revealed that Mage-D1 is expressed throughout the process of tooth germ development and that Mage-D1 plays a key role in the proliferation, migration and differential mineralization of EMSCs. The potential mechanism of Mage-D1 involvement in differential mineralization seems to be related to p75NTR, Dlx1 and Msx1.

Mage-D1 expression is regulated by strong posttranscriptional regulation during murine embryogenesis and presents spatiotemporal tissue specificity<sup>24</sup>. However, the expression of Mage-D1 in tooth germs has not yet been clearly elucidated, so our research investigated it first. As the results showed, Mage-D1 was strongly expressed in the proliferative epithelium and the budding enamel apparatus at E12.5 d, which suggested that Mage-D1 may be connected with the initiation of tooth development. The expression of Mage-D1 in dental papilla began at the bell stage, a mature stage of glazer. During this period, the cells in different parts have specific phenotypes and have the ability to form corresponding tooth tissues. Mage-D1 was strongly expressed in the inner enamel epithelium, outer enamel epithelium, and cervical loop, which suggested that Mage-D1 may be involved in epithelial-mesenchymal mineralization and dental signal interaction in early tooth development. Then, the outer layer cells of dental papilla differentiated into high columnar odontoblasts to form mineralized dentin in the future. The expression of Mage-D1 increased continuously and was strongly expressed in ameloblasts, odontoblasts, dental follicle cells, and alveolar bone osteoblasts, which suggested that Mage-D1 may be associated with the mineralization of enamel and dentin. Mage-D1 is widely expressed in epithelial root sheath at PN4, which suggests that Mage-D1 may also be involved in the development of roots. During the development of tooth germ, Mage-D1 was slight expressed in the cells at the centre area of the dental papilla. Therefore, whether Mage-D1 participates in the formation of dental pulp may need further exploration. In short, the above studies showed that Mage-D1 was expressed with temporal and spatial specificity in tooth germ development.

EMSCs provide a profitable in vitro stem cell model for the study of tooth morphogenesis<sup>12</sup>. The enamel organ entered a mature stage at E19.5, the late bell-shaped stage. Histological results showed that the expression of Mage-D1 in tooth germ was at a high level at E19.5 d, which was more suitable for studying the regulatory function of Mage-D1 in vitro. In addition, P75NTR, as a marker for isolated cranial neural crest-derived EMSCs<sup>25</sup>, was expressed at a high rate and with higher purity in E19.5 d EMSCs<sup>5</sup>. So in this study, EMSCs were extracted from foetal rats at E19.5 d SD.

The migration and proliferation of EMSCs are important for epithelial-mesenchymal transfer and metabolism during tooth development and involve many gene-regulating processes. Our studies showed that Mage-D1 can inhibit the migration of EMSCs, which is consistent with the migration inhibition result of Mage-D1 in glioma stem cells<sup>26</sup>, human breast cancer cells<sup>27</sup>, HeLa cells<sup>28</sup>, melanoma or pancreatic cancer cells<sup>29</sup> and many other tumour cells. Cell migration is a critical physiological event associated with four other main cellular processes: adhesion, proliferation, differentiation, and death. Wu et al. reported that Mage-D1 can suppress the differentiation of mouse dental papilla cell-23(MDPC-23) cells and odontoblast-lineage cell (OLCs) by interrupting the premature formation of dentin<sup>22</sup>. The migration inhibition effect of Mage-D1 in EMSCs may affect the stages of dentin differentiation or other processes, followed by affecting the development of teeth. Moreover, Mage-D1 can promote the proliferation of EMSCs, which is similar to the effect of Mage-D1 on the proliferation of dental pulp cells revealed by Qi et al<sup>21</sup>. Jiang et al. also indicated that interference with Mage-D1 expression could reduce the proliferation of human gastric cancer cell lines<sup>30</sup>. In oesophageal carcinomas, Mage-D1 accelerates cell proliferation by stabilizing proliferating cell nuclear antigen (PCNA) in a ubiquitin–proteasome pathway<sup>31</sup>. Mage-D1 can interact with a variety of proteins with different functions<sup>14</sup>. For example, the interaction of p75NTR can regulate apoptosis<sup>32</sup>, the interaction of p53 can regulate the cell cycle<sup>33</sup>. It is not surprising that the roles of Mage-D1 vary because of cell type specificity<sup>34</sup>. We also found that a large number of subjects showed the inhibitory proliferative effect of Mage-D1; for instance, Mage-D1 inhibited the proliferation of breast cancer cells when ectopically expressed<sup>35</sup>. Some studies also indicated that the protein complex with Mage-D1, Dlx5 and Necdin could arrest the proliferation of osteogenic cells<sup>36</sup>. In short, the impact of Mage-D1 on the proliferation and migration of EMSCs is closely related to tooth development.

Mage-D1 is expressed in adherent cells rather than haematopoietic cells in bone, including osteoblastic and chondrogenic cells<sup>37</sup>. Our research also found that Mage-D1 is strongly expressed in various mineralization-related cells during the development of dental embryos. We further investigated the regulatory role of Mage-D1 in mineralization and tooth formation. Dspp belongs to dentin-specific proteins<sup>38</sup>. Dmp1, BSP, and OPN are mineralized tissue-specific proteins, and they play important roles in inducing cell differentiation and promoting dentin mineralization. Col-1 and Runx2 proteins are predominantly expressed during the earlier phases of proliferation and maturation, and ALP and OPN are expressed after the middle phase<sup>4</sup>. All of them play considerable roles in differential mineralization during the developmental stages of teeth and maxillofacial structures<sup>5</sup>. The protein and gene expression levels of relevant mineralization and odontogenic factors were increased in EMSCs after overexpression

of Mage-D1, and the above results were reversed after silencing Mage-D1, which suggested that Mage-D1 positively regulated osteogenic differentiation in rat EMSCs. Gina et al. observed remarkable decreased bone mineral density (BMD) in Mage-D1-deficient mice<sup>39</sup>. Both bone tissue and teeth are mineralized tissues, so there are many commonalities in their biological characteristics and matrix formation. In human osteosarcoma cells (MG63 cells), the expression of Runx2 was concurrently increased with Dlx5, Mage-D1 and Nectin. However, some mineralization experiments proposed that Mage-D1 knockdown promoted the mineralization potential of mouse dental papilla cell (mDPCs)<sup>21</sup>. This may be related to the different regulatory roles exhibited by Mage-D1 in different cells. Mage-D1 can change its cellular localization under the stimulation of some factors; for example, the interaction of nerve growth factor (NGF) with p75NTR was responsible for the translocation of Mage-D1 from the cytoplasm to the cell membrane<sup>40</sup>, which represents the diverse functions of Mage-D1. A study by Liu et al. showed that the knockdown of Mage-D1 induced autophagy-related gene expression and boosted the process of periodontitis by enhancing osteoclast activity and differentiation<sup>23</sup>. Therefore, we boldly speculate that the role of Mage-D1 in osteogenesis varies with cell type, which suggesting the complex and diverse roles of Mage-D1 in osteogenesis and odontogenesis.

The expression of Mage-D1 in the mature rat brain was similar to that of p75NTR, but Mage-D1 was more widely distributed, suggesting that Mage-D1 may also participate in other signalling pathways<sup>41</sup>. Moreover, in mouse tooth germ, Mage-D1 was intensity expressed in the dental sac, dental papilla and inner enamel epithelium, analogous to that of p75NTR, which implied that Mage-D1 might be associated with P75NTR during tooth development<sup>6</sup>. The Dlx/Msx family has been shown to play a role in tooth development and regulate mineralization-related genes<sup>42-44</sup>. Msx1 participates in initial tooth embryogenesis and regulates the proliferation and differentiation of mouse dental mesenchymal cells<sup>45</sup>. The presence of Dlx1 is a key factor for normal tooth development, especially for the development of maxillary molars<sup>46</sup>. It is amazing that most Dlx/Msx family proteins are connected with Mage-D1. Mage-D1 may be a common transcriptional regulator mediated by Dlx/Msx homologous domain proteins<sup>37,47</sup>. Our coimmunoprecipitation results verified that Mage-D1 could bind to p75NTR, Dlx1 and Msx1 with EMSCs as the cell model. Ultimately, the protein and gene levels of p75NTR, Dlx1, and Msx1 were significantly increased after overexpression of Mage-D1, and the opposite results were obtained after silencing. p75NTR is a membrane receptor protein, and Dlx1 and Msx1 are intranuclear transcription factors. Mage-D1, a significant protein that can change subcellular localization and expression levels in response to external signal stimulation, may transmit signals from outside the cell to transcriptional proteins in the plasmatic nucleus by binding to the three proteins; therefore, a series of cellular activities are triggered. Thus, we hypothesize that the involvement of Mage-D1 in the regulation of tooth development may be closely related to the binding and signalling of Mage-D1, which may be affected by both Mage-D1 protein expression and intracellular localization, but the specific signalling mechanism needs to be explored further. Previous studies speculated that Mage-D1 acts as a bridge between p75NTR and Dlx/Msx<sup>5,6</sup>. Our study further shows that the relationship between Mage-D1 and p75NTR is not only a simple upstream-downstream relationship, but more like a synergistic and mutually restraining

relationship. It can be seen that the mechanism by which Mage-D1 is involved in tooth development is diverse and complex.

In summary, our studies pointed out that Mage-D1 was differentially expressed in time and space during tooth development and negatively regulated the migration of EMSCs but positively regulated the proliferation and mineralization of EMSCs. Further studies suggested that Mage-D1 may be closely related to p75NTR, Dlx1 and Msx1 in tooth development. Taken together, our results show that Mage-D1 is absolutely necessary in tooth germ development. This novel finding may prompt future studies devoted to exploring how Mage-D1 functions and use of its molecular mechanism in dental histological engineering.

## Materials And Methods

**Experimental animals.** Sprague–Dawley (SD) rats were acquired from Chongqing Medical University Animal Laboratory in this study. The existence of a vaginal plug was treated as E 0.5 d. One day after birth was recorded as PN1. All experiments were conducted in accordance with the scheme approved by the Ethics Committee of the Affiliated Stomatological Hospital of Chongqing Medical University, including any relevant details, and we confirmed that all experiments were performed in accordance with relevant guidelines and regulations.

**HE and immunohistochemistry staining.** The SD rat embryo heads or maxillas of E12.5 d, E15.5 d, E19.5 d, PN1, and PN4 (n = 3 each group) were collected and fixed with 4% paraformaldehyde (Solarbio, Beijing, China) for 24 h. The maxilla samples were demineralized with ethylenediaminetetraacetic acid (EDTA) decalcifying solution (Solarbio). Then, the samples were dehydrated by alcohol, embedded in paraffin and sliced into 5 µm tissue sections. HE staining was carried out according to the manufacturer's protocols (Solarbio). For immunostaining, briefly, the slides were blocked with goat serum (Bioss, Beijing, China) and then incubated with the rabbit polyclonal antibody to Mage-D1 (1:100, Biorbyt, Cambridgeshire, British) at 4°C overnight. Next day, the slides were incubated with an anti-rabbit secondary antibody (1:3000, Bioss), followed by colouring with diaminobenzidine (DAB) (Zsbio, Beijing, China). Finally, cell nuclei were counterstained with haematoxylin (Solarbio). Scanning and analysis of staining results were performed with a scanner.

**Isolation and culture of E19.5 d EMSCs.** The isolation and culture of E19.5 d EMSCs were carried out as previously described.<sup>1,5</sup> The embryonic maxillofacial process of E19.5 d SD embryo rats was dissected, and the maxillary tooth germ was taken. The minced tissue was placed directly in a sterile petridish using the tissue block adherence method. Then, the culture medium (composed of 89% Dulbecco's modified eagle medium/F12 (Sigma, Darmstadt, Germany), 10% foetal bovine serum (Ausgenex, Gold Coast, Australia) and 1% penicillin-streptomycin liquid (Solarbio)) was gently added and cultured in a humidified incubator at 37°C and 5% CO<sub>2</sub> for approximately 3 days. After the cells had fully crawled out, routine follow-up cell passaging treatments were carried out.



**Phalloidin staining.** After the cells reached 70% confluence in a six-well plate, they were fixed with 4% paraformaldehyde for 30 minutes, and then 0.1% Triton X-100 (Solarbio) was added to break the membrane for 20 minutes. Approximately 100 microlitres of phalloidin working solution (Sigma) was added, followed by incubation for 2 h at room temperature. The cell nucleus was stained with 4',6-diamidino-2-phenylindole dihydrochloride solution (DAPI) (Solarbio) and incubated for 10 min in the dark. Finally, the cytoskeleton was observed with a confocal laser scanning microscope (CLSM) (Leica, Heidelberg, Germany).

**Flow cytometry identification.** Approximately  $5 \times 10^5$  cells were collected in each group, and then we detected cell surface markers by flow cytometry. The cells were fixed with 4% polyoxymethylene for 15 minutes, and then primary antibodies (mouse monoclonal antibody to CD44, CD29, CD90, CD105 and CD146) (1:100; Santa Cruz Biotechnology, Texas, USA) were added and incubated overnight at 4°C. The anti-mouse secondary antibody (1:100, Bioss) was added the next day and incubated for at least one hour. The cells were then analysed by flow cytometry.

**Transfection of Mage-D1-overexpressing and Mage-D1-silenced plasmids.** The full-length coding region of rat Mage-D1 was amplified by PCR and cloned into the vector pLVX-puro for expression. The specific primers were as follows: 5'-ACACTCGAGATGGCTCAGAAACCGGACGGCG-3' (forward) and 5'-CTGAAT TCTTACTCAACCCAGAAGAAGCCAATGGCACCG-3' (reverse). The plasmids were cotransfected with psPAX2 and pCMV-VSV-G packaging plasmids into HEK-293T cells with active growth by Lipofectamine 2000 (Invitrogen, Massachusetts, USA). The virus-containing supernatant was collected at 2 to 3 days after transfection, which was used to infect the target cells, and 8 µg/ml polybutene (Solarbio) was added. After at least 24 hours, the target cells were continuously screened for 10 days with 4 µg/ml puromycin (Solarbio) for further research. To knock down the expression of endogenous Mage-D1, plasmids were established with pLKO.1. The sequences were as follows: 5'-AAGGTGGCCTTTAAGTCACAG-3'. The packaging of these knockdown lentiviruses is similar to that of overexpression lentiviruses.

**Immunofluorescence staining.** The transfected cells were plated on a cell slide until the cells reached 70% confluence and then fixed with 4% paraformaldehyde, followed by incubation with the rabbit polyclonal antibody to Mage-D1 (1:100, Biorbyt) overnight at 4°C. The anti-rabbit secondary antibody (1:100, Bioss) was added the next day and incubated at room temperature for 30 minutes. The cell nuclei were counterstained with DAPI and observed under CLSM.

**CCK-8 proliferation and scratch test.** Briefly, the transfected EMSCs were seeded in a 96-well plate at  $2 \times 10^3$  cells/well (Corning). Starting on the second day, we detected cell proliferation by using the CCK-8 assay for 8 consecutive days according to the manufacturer's instructions. The number of viable cells in each well was determined by measuring the absorbance at 450 nm wavelength with a microplate reader. Cell proliferation was expressed as the mean  $\pm$  standard deviation of the absorbance of 5 wells in each group. The transfected cells were spread in a six-well plate until full. Then, we changed to serum-free medium and used a 200 µL pipette tip to mark the inside of the well plate and cultured the cells in a

humidified incubator at 37°C and 5% CO<sub>2</sub>. Photos were taken at 0, 24, and 48 h. ImageJ software was used to analyse cell migration area ratio in each group.

**Real-time PCR assay.** General RNA of every group of cells was obtained by Trizol reagent (Invitrogen) and then reverse transcribed with a kit (TaKaRa, Kusatsu, Japan). The quantities of RNA and cDNA were detected with an ultraviolet spectrophotometer. Quantitative real-time PCR was carried out by using SYBRII qPCR master mix reagent (TaKaRa) and run with a 20 µl reaction system. There were at least 3 secondary wells per group. At the same time, the GAPDH gene was used as a control. Primer information for related genes is shown in Supplementary Table 1.

**Co-immunoprecipitation (Co-IP) and WB.** Total cell proteins were retrieved with cell lysis buffer (Beyotime), and the protein level was measured by the BCA kit (Bioworld, Beijing, China). For coimmunoprecipitation, first, the magnetic beads (Biorad, California, USA) were incubated with rabbit polyclonal antibody to Mage-D1 (1:200, Proteintech, Chicago, USA) for 2 hours, followed by the addition of protein lysate and incubation overnight at 4°C. The unreacted proteins were separated magnetically and discarded the next day. Western blot was conducted as described previously. The protein samples were separated by SDS–PAGE and transferred to PVDF membranes (Pierce, Dallas, USA). Primary antibodies against Mage-D1 (1:1000; Biorbyt), p75NTR (1:1000, Cell Signaling Technology, Poston, USA), Runx2 (1:1000, CST), BSP II (1:1000, CST), Dlx1 (1:200, Biorbyt), Msx1 (1:200, Biorbyt), and GAPDH (1:1000, CST) were used as internal standards. On the second day, the membranes were incubated with anti-rabbit or anti-mouse secondary antibody (1:5000, Bioss) for two hours at room temperature. Finally, the signal was revealed with BeyoECL Plus solution (Beyotime).

**Statistical analysis.** Total data are shown as the mean ± standard deviation (SD). Statistical significance was determined with SPSS 20.0 software (IBM Analytics, Armonk, NY, USA). Statistical comparisons were made by Student's t test and one-way analysis of variance (ANOVA). Differences were statistically significant when  $p < 0.05$ .

## Declarations

### Acknowledgements

This study was supported by the National Natural Science Foundation of China (Grant no. 81970906). All the experiments were performed in the Chongqing Key Laboratory of Oral Diseases and Biomedical Sciences.

### Author contributions

M.L. designed the research, conducted the experiments and wrote the paper. X.Y. and Y.L. conducted the experiments. H.Y. and Y.Z. performed the data analyses and edited the manuscript. X.W. and Z.Z. designed the research, supervised the study, and wrote the manuscript. All authors reviewed the manuscript.

## Data Availability

All data generated or analysed during this study are included in this published article and its supplementary information files.

## Competing interests

The authors declare no competing interests.

## Statement

The study is reported in accordance with ARRIVE guidelines.

## References

1. Zhao M, et al. The spatiotemporal expression and mineralization regulation of p75 neurotrophin receptor in the early tooth development. *Cell Prolif.* **52**, e12523, (2019).
2. Thesleff I, Sharpe P. Signalling networks regulating dental development. *Mech Dev.* **67**, 111–23, (1997).
3. Li J, Parada C, Chai Y. Cellular and molecular mechanisms of tooth root development. *Development.* **144**, 374–384, (2017).
4. Di Certo MG, et al. NRAGE associates with the anti-apoptotic factor Che-1 and regulates its degradation to induce cell death. *J Cell Sci.* **120**, 1852–8, (2007)
5. Yang K, et al. p75 neurotrophin receptor regulates differential mineralization of rat ectomesenchymal stem cells. *Cell Prolif.* **50**, e12290, (2017).
6. Zhao M, et al. The role and potential mechanism of p75NTR in mineralization via in vivo p75NTR knockout mice and in vitro ectomesenchymal stem cells. *Cell Prolif.* **53**, e12758, (2020).
7. Pöld M, et al. Identification of a new, unorthodox member of the MAGE gene family. *Genomics.* **59**, 161–7, (1999).
8. Sasaki A, Hinck L, Watanabe K. RumMAGE-D the members: structure and function of a new adaptor family of MAGE-D proteins. *J Recept Signal Transduct Res.* **25**, 181–98, (2005).
9. Mouri A, Noda Y, Watanabe K, Nabeshima T. The roles of MAGE-D1 in the neuronal functions and pathology of the central nervous system. *Rev Neurosci.* **24**, 61–70, (2013).
10. Barker PA, Salehi A. The MAGE proteins: emerging roles in cell cycle progression, apoptosis, and neurogenetic disease. *J Neurosci Res.* **67**, 705–12, (2002).
11. Zhang G, Zhou H, Xue X. Complex roles of NRAGE on tumor. *Tumour Biol.* **37**, 11535–11540, (2016).
12. Kuwajima T, Nishimura I, Yoshikawa K. Necdin promotes GABAergic neuron differentiation in cooperation with Dlx homeodomain proteins. *J Neurosci.* **26**, 5383–92, (2006).
13. Sasaki A, Masuda Y, Iwai K, Ikeda K, Watanabe K. A RING finger protein Praja1 regulates Dlx5-dependent transcription through its ubiquitin ligase activity for the Dlx/Msx-interacting

- MAGE/Necdin family protein, Dlxin-1. *J Biol Chem.* **277**, 22541–6, (2002).
14. Yang Q, et al. NRAGE promotes cell proliferation by stabilizing PCNA in a ubiquitin-proteasome pathway in esophageal carcinomas. *Carcinogenesis.* **35**, 1643–51, (2014).
  15. Kumar S, et al. A pathway for the control of anoikis sensitivity by E-cadherin and epithelial-to-mesenchymal transition. *Mol Cell Biol.* **31**, 4036–51, (2011).
  16. Bertrand MJ, et al. NRAGE, a p75<sup>NTR</sup> adaptor protein, is required for developmental apoptosis in vivo. *Cell Death Differ.* **15**, 1921–9, (2008).
  17. Williams ME, Strickland P, Watanabe K, Hinck L. UNC5H1 induces apoptosis via its juxtamembrane region through an interaction with NRAGE. *J Biol Chem.* **278**, 17483–90, (2003).
  18. Lai SS, et al. Ror2-Src signaling in metastasis of mouse melanoma cells is inhibited by NRAGE. *Cancer Genet.* **205**, 552–62, (2012).
  19. Feng Z, Li K, Liu M, Wen C. NRAGE is a negative regulator of nerve growth factor-stimulated neurite outgrowth in PC12 cells mediated through TrkA-ERK signaling. *J Neurosci Res.* **88**, 1822–8, (2010).
  20. Liu L, et al. Knockdown of *NRAGE* Impairs Homologous Recombination Repair and Sensitizes Hepatoblastoma Cells to Ionizing Radiation. *Cancer Biother Radiopharm.* **35**, 41–49, (2020).
  21. Qi S, et al. Effects of neurotrophin receptor-mediated MAGE homology on proliferation and odontoblastic differentiation of mouse dental pulp cells. *Cell Prolif.* **48**, 221–30, (2015).
  22. Wu Q, et al. Knockdown of NRAGE induces odontogenic differentiation by activating NF- $\kappa$ B signaling in mouse odontoblast-like cells. *Connect Tissue Res.* **60**, 71–84, (2019).
  23. Liu H, et al. Knockout of NRAGE promotes autophagy-related gene expression and the periodontitis process in mice. *Oral Dis.* **27**, 589–599, (2021).
  24. Kendall SE, Goldhawk DE, Kubu C, Barker PA, Verdi JM. Expression analysis of a novel p75<sup>(NTR)</sup> signaling protein, which regulates cell cycle progression and apoptosis. *Mech Dev.* **117**, 187–200, (2002).
  25. Li G, et al. SOST, an LNGFR target, inhibits the osteogenic differentiation of rat ectomesenchymal stem cells. *Cell Prolif.* **51**, e12412, (2018).
  26. Wen X, et al. Characterization of p75<sup>(+)</sup> ectomesenchymal stem cells from rat embryonic facial process tissue. *Biochem Biophys Res Commun.* **427**, :5–10, (2012).
  27. Reddy EM, et al. Dlxin-1, a member of MAGE family, inhibits cell proliferation, invasion and tumorigenicity of glioma stem cells. *Cancer Gene Ther.* **18**, 206–18, (2011).
  28. Du Q, Zhang Y, Tian XX, Li Y, Fang WG. MAGE-D1 inhibits proliferation, migration and invasion of human breast cancer cells. *Oncol Rep.* **22**, 659–65, (2009).
  29. Shen WG, et al. Melanoma-associated antigen family protein-D1 regulation of tumor cell migration, adhesion to endothelium, and actin structures reorganization in response to hypoxic stress. *Cell Commun Adhes.* **14**, 21–31, (2007).
  30. Chu CS, et al. NRAGE suppresses metastasis of melanoma and pancreatic cancer in vitro and in vivo. *Cancer Lett.* **250**, 268–75, (2007).

31. Jiang X, Jiang X, Yang Z. NRAGE confers poor prognosis and promotes proliferation, invasion, and chemoresistance in gastric cancer. *Gene*. **668**, 114–120, (2018).
32. Shimizu D, et al. NRAGE promotes the malignant phenotype of hepatocellular carcinoma. *Oncol Lett*. **11**, 1847–1854, (2016).
33. Salehi AH, Xanthoudakis S, Barker PA. NRAGE, a p75 neurotrophin receptor-interacting protein, induces caspase activation and cell death through a JNK-dependent mitochondrial pathway. *J Biol Chem*. **277**, 48043–50, (2002).
34. Wen CJ, et al. hNRAGE, a human neurotrophin receptor interacting MAGE homologue, regulates p53 transcriptional activity and inhibits cell proliferation. *FEBS Lett*. **564**, 171–6, (2004).
35. Passananti C, Fanciulli M. The anti-apoptotic factor Che-1/AATF links transcriptional regulation, cell cycle control, and DNA damage response. *Cell Div*. **J2:21**, (2007).
36. Ju H, Lee S, Lee J, Ghil S. Necdin modulates osteogenic cell differentiation by regulating Dlx5 and MAGE-D1. *Biochem Biophys Res Commun*. **489**, 109–115, (2017).
37. Masuda Y, et al. Dlxin-1, a novel protein that binds Dlx5 and regulates its transcriptional function. *J Biol Chem*. **276**, 5331–8, (2001).
38. Huang X, et al. Dentinogenesis and Tooth-Alveolar Bone Complex Defects in *BMP9/GDF2* Knockout Mice. *Stem Cells Dev*. **28**, 683–694, (2019).
39. Calabrese G, et al. Systems genetic analysis of osteoblast-lineage cells. *PLoS Genet*. **8**, e1003150, (2012).
40. Frade JM. NRAGE and the cycling side of the neurotrophin receptor p75. *Trends Neurosci*. **23**, 591–2, (2000).
41. Barrett GL, Greferath U, Barker PA, Trieu J, Bennie A. Co-expression of the P75 neurotrophin receptor and neurotrophin receptor-interacting melanoma antigen homolog in the mature rat brain. *Neuroscience*. **133**, 381–92, (2005).
42. Lézot F, et al. Biomineralization, life-time of odontogenic cells and differential expression of the two homeobox genes MSX-1 and DLX-2 in transgenic mice. *J Bone Miner Res*. **15**, 430–41, (2000).
43. Satokata I, Maas R. Msx1 deficient mice exhibit cleft palate and abnormalities of craniofacial and tooth development. *Nat Genet*. **6**, 348–56, (1994).
44. Chen Y, Bei M, Woo I, Satokata I, Maas R. Msx1 controls inductive signaling in mammalian tooth morphogenesis. *Development*. **122**, 3035–44, (1996).
45. Feng XY, Zhao YM, Wang WJ, Ge LH. Msx1 regulates proliferation and differentiation of mouse dental mesenchymal cells in culture. *Eur J Oral Sci*. **121**, 412–20, (2013).
46. Thomas BL, et al. Role of Dlx-1 and Dlx-2 genes in patterning of the murine dentition. *Development*. **124**, 4811–8, (1997).
47. Kuwajima T, Taniura H, Nishimura I, Yoshikawa K. Necdin interacts with the Msx2 homeodomain protein via MAGE-D1 to promote myogenic differentiation of C2C12 cells. *J Biol Chem*. **279**, 40484–93, (2004).

# Figures

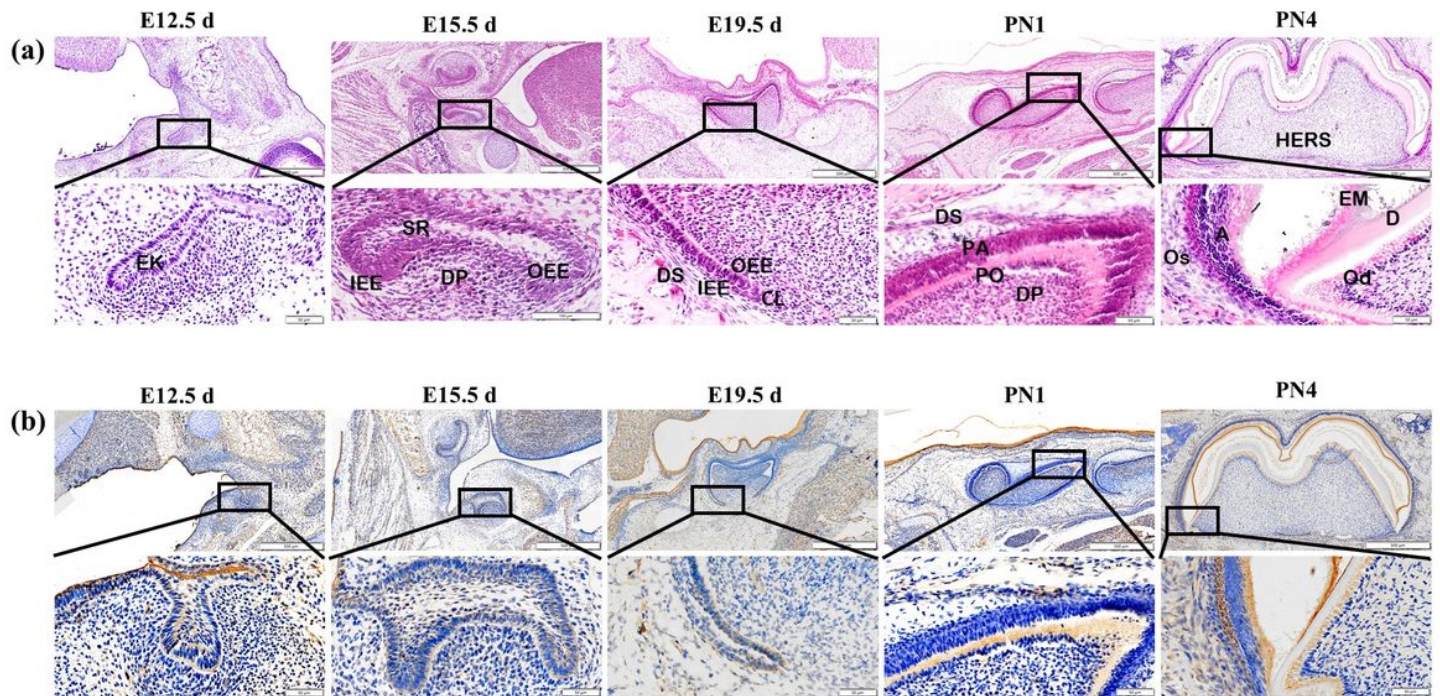


**Figure 1**

The results of HE staining and expression pattern of Mage-D1 in the stage of rat tooth germ development. (a) HE staining of first mandibular molar in rat at E12.5 d, E15.5 d, E19.5 d, PN1, PN4. (b) Mage-D1 expression in first molar of rat at E12.5 d, E15.5 d, E19.5 d, PN1 and PN4 by immunohistochemistry. Scale bars: 50  $\mu$ m or 500  $\mu$ m. EK, enamel organ; SR, stellate reticulum; IEE, inner enamel epithelium; OEE, outer enamel epithelium; DP, dental papilla; DS, dental sac; CL, cervical loop; PA, preameloblasts; PO, predontoblast; HERS, Hertwig's epithelial root sheath; A, ameloblasts; D, Dentin; EM, Enamel matrix; Od, odontoblast; Os, osteoblast.

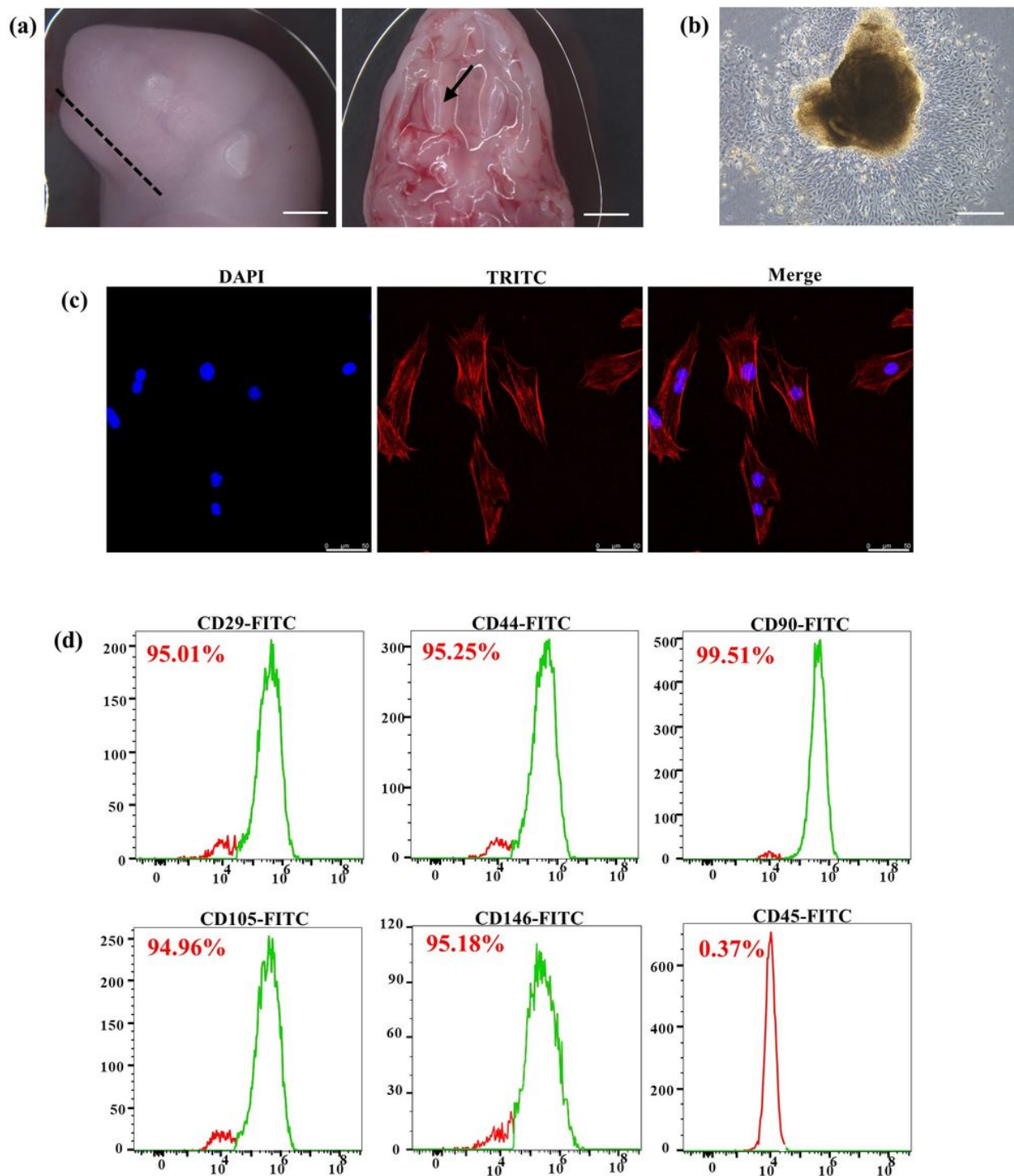


**Figure 2**

Isolation and characterization of rat embryonic EMSCs. (a) The E19.5 d SD rat embryo head and maxillary process. Scale bars: 2.5 mm. (b) The E19.5 d EMSCs. Scale bars: 250  $\mu$ m. (c) Phalloidin staining of E19.5 d EMSCs. Scale bars: 50  $\mu$ m. (d) The MSC markers CD29, CD44, CD90, CD105, and CD146 were strongly expressed in EMSCs, while the hematopoietic marker CD45 was hardly detected.

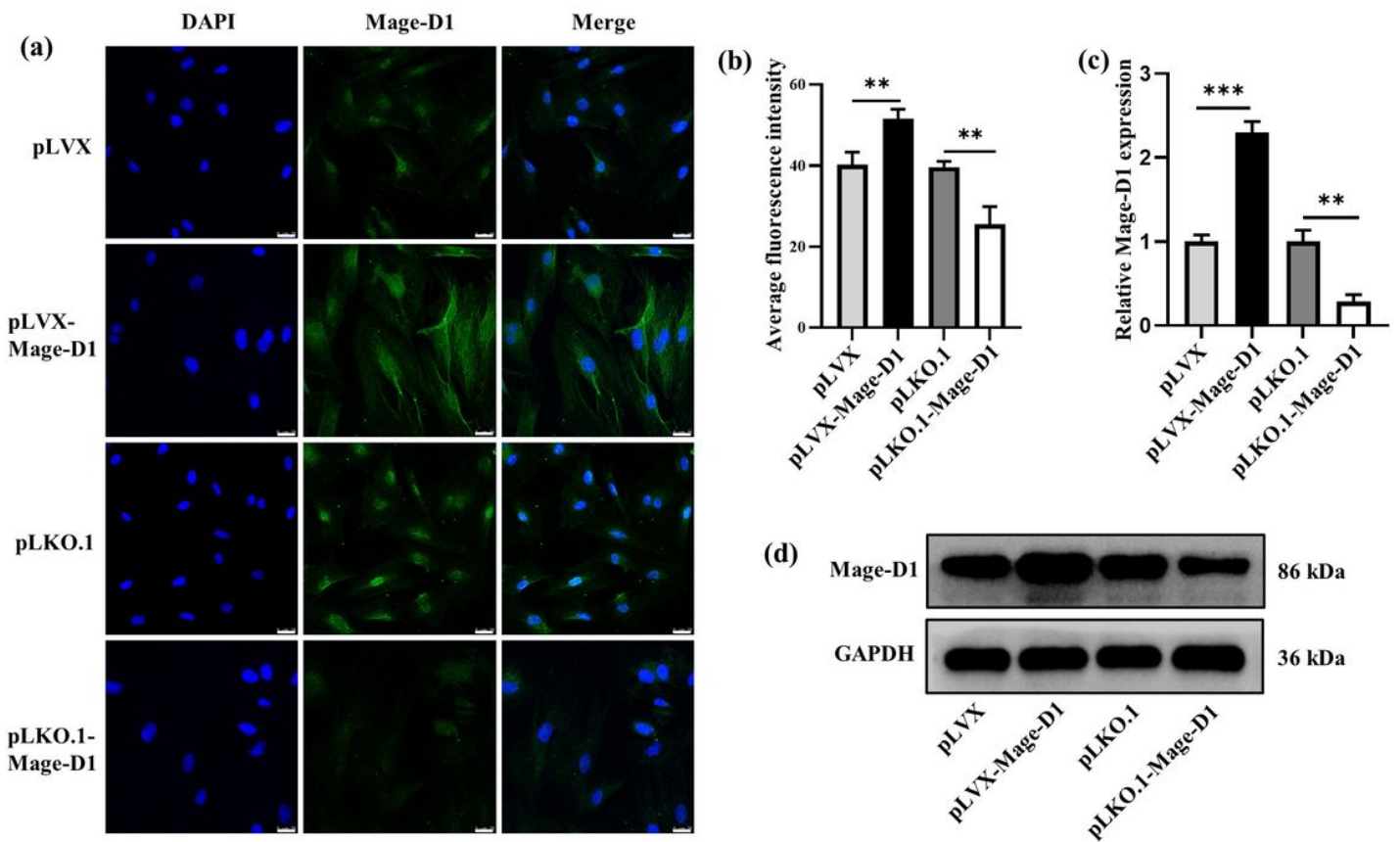


**Figure 3**

After transfection of E19.5 d EMSCs with Mage-D1 overexpression and silencing plasmids. (a) Immunofluorescence staining of empty plasmid (pLVX group), transfection with Mage-D1 overexpression plasmid pLVX (pLVX Mage-D1 group), empty plasmid (pLKO.1 group) and transfection with Mage-D1 silencing plasmid pLKO.1 (pLKO.1-Mage-D1 group); scale bar represents 25  $\mu$ m. (b) Immunofluorescence quantitative statistics of (a), statistics are presented in Supplementary Figure S1 and Supplementary Table 2. (c) After transfection of cells with lentivirus, the expression levels of Mage-D1 were examined by real-time PCR normalized to GAPDH. For raw data see Supplementary Table 3. (d) After transfection of cells with lentivirus, the expression levels of Mage-D1 were detected by Western blot analysis, GAPDH used as the reference gene. Full-length blots are presented in Supplementary Figure S2. (\*\* $P < 0.01$ , \*\*\* $P < 0.001$ ).



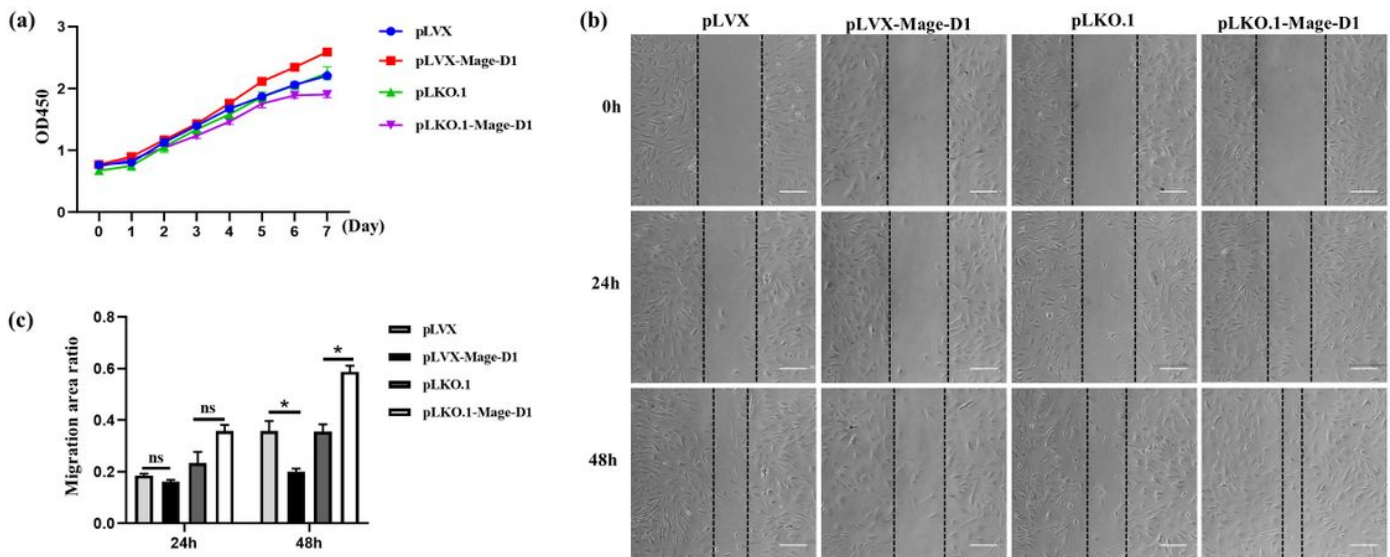


**Figure 4**

Regulation of Mage-D1 influence the proliferation capacities and migration capacities of E19.5 d EMSCs. (a) The proliferation rate was assessed by CCK-8 cultured for 8 days. For raw data see Supplementary Table 4. (b) The migration rate was assessed for two consecutive days. Scale bar represents 250 μm. (c) The migration rate quantitative statistics of (b). For raw data see Supplementary Figure S3 and Supplementary Table 5. (ns represents no significance,  $*P < 0.05$ ).

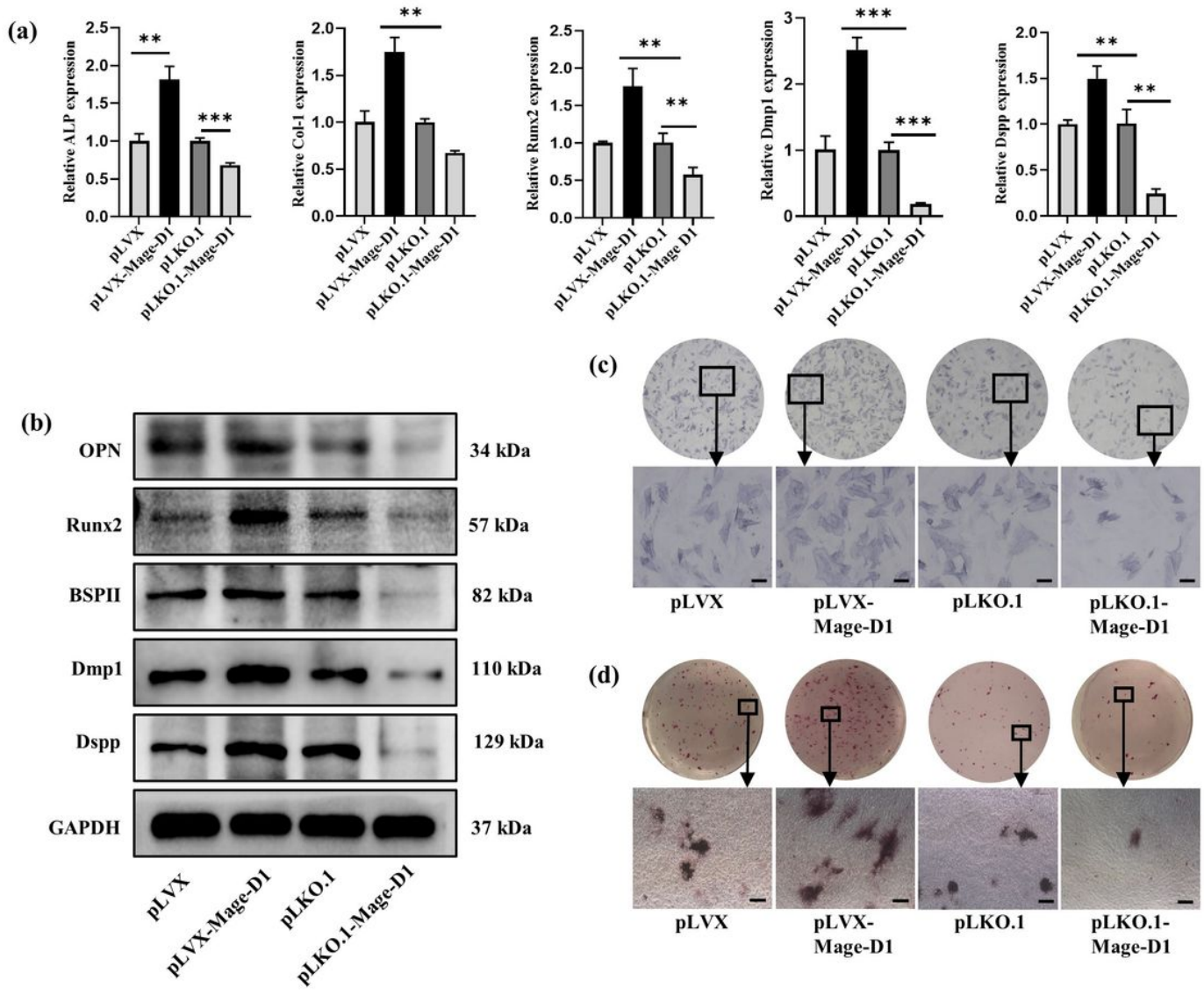


**Figure 5**

Overexpression and silencing of Mage-D1 affects the mineralization regulation of E19.5 d EMSCs. (a) Under induction with mineralized culture medium for 7 d, the expression levels of ALP, Runx2, Col-1, Dmp1, Dspp were examined by real-time PCR normalized to GAPDH. For raw data see Supplementary Table 3. (b) Under induction with mineralized culture medium for 14 d, the expression levels of OPN, Runx2, BSP, Dmp1, Dspp were detected by Western blot analysis, GAPDH used as the reference gene. Full-length blots are presented in Supplementary Figure S4. (c) Under induction with mineralized culture medium for 14 d, ALP staining was used to detect their potential of differential mineralization. Scale bar represents 50 μm. (d) Under induction with mineralized culture medium for 21 d, alizarin red staining was used to detect their mineralized nodules. Scale bar represents 200 μm. (\*\* $P < 0.01$ , \*\*\* $P < 0.001$ ).

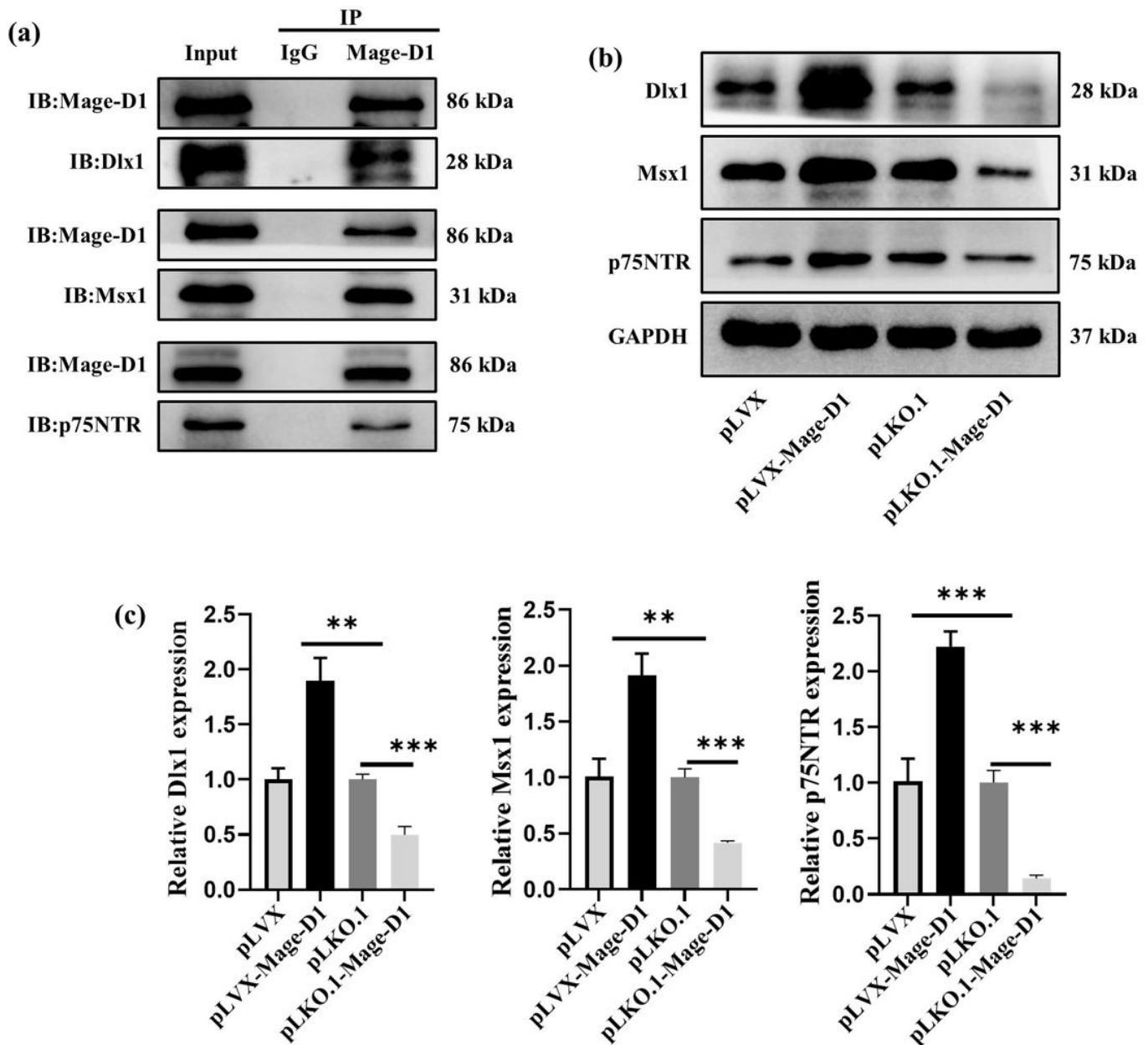


**Figure 6**

Investigations revealing the potential mechanism of Mage-D1 in mineralization. (a) Co-immunoprecipitation shows that Mage-D1 can bind to p75NTR, Msx1, Dlx1 based on E19.5 d EMSCs. Full-length blots are presented in Supplementary Figure S5. (b) Under induction with mineralized culture medium for 14 d, the expression levels of p75NTR, Msx1, Dlx1 were detected by Western blot analysis, GAPDH used as the reference gene. Full-length blots are presented in Supplementary Figure S6. (c) Under induction with mineralized culture medium for 7 d, the expression levels of p75NTR, Msx1, Dlx1 were examined by real-time PCR normalized to GAPDH. For raw data see Supplementary Table 3. (\*\* $P < 0.01$ , \*\*\* $P < 0.001$ ).

## Supplementary Files

This is a list of supplementary files associated with this preprint. Click to download.

- [Supplementarymaterial.docx](#)
- [SupplementaryTable2.xlsx](#)
- [SupplementaryTable3.xlsx](#)
- [SupplementaryTable4.xlsx](#)
- [SupplementaryTable5.xlsx](#)